

Jarosite-type precipitates mediated by YN22, *Sulfobacillus thermosulfidooxidans*, and their influences on strain

DING Jian-nan(丁建南), GAO Jian(高 健), WU Xue-ling(吴学玲),
ZHANG Cheng-gui(张成桂), WANG Dian-zuo(王淀佐), QIU Guan-zhou(邱冠周)

School of Resources Processing and Bioengineering, Central South University, Changsha 410083, China

Received 25 December 2006; accepted 29 April 2007

Abstract: To have a better understanding on the properties of the jarosite-type precipitate synthesized by *Sulfobacillus thermosulfidooxidans*, the evolution of the *S. thermosulfidooxidans*-mediated precipitation and the influence of the precipitate on this species, a newly isolated strain (YN22) of *S. thermosulfidooxidans* was cultured in a medium containing Fe^{2+} as energy source under optimal conditions (pH 1.5, 53 °C, 0.2 g/L yeast extract, 30 g/L $\text{Fe}_2\text{SO}_4 \cdot 7\text{H}_2\text{O}$ and 170 r/min), added with or without glass beads. Remarkable differences were found in the oxidation rate of Fe^{2+} , the precipitate yield of jarosite-type compounds and the population density between the two groups of cultures. The group with glass beads has a 6 h faster Fe^{2+} oxidation, 6 h earlier precipitation, 78% higher precipitate yield and much lower population density than those without glass beads. XRD, EDS, FTIR and SEM analysis reveals that the precipitates originated from both groups are a mixture of potassium jarosite and ammoniojarosite, with morphological features similar to the latter. The results of the test referring to influence of the precipitates on YN22 show that the precipitate from the group without glass beads has no apparent influence on Fe^{2+} oxidation rate of YN22 and only a limited influence on growth of the strain, whereas that from the group with glass beads remarkably inhibits the growth and Fe^{2+} oxidation ability of YN22 when a precipitate content over 4 g/L is used.

Key words: strain YN22; *Sulfobacillus thermosulfidooxidans*; precipitate; jarosite; ammoniojarosite

1 Introduction

Microbial hydrometallurgy is deemed more environmentally friendly and economical than conventional pyrometallurgy[1–3]. Recovering metal from sulphide minerals by acidophiles has developed into a successful and expanding area of biotechnology. Mesophilic acidophiles, such as *Acidithiobacillus ferrooxidans*, are the most widely used leaching microbes in the processing of metal ores. However, compared with thermophilic acidophiles, they always require much longer time for mineral processing and are less thermotolerant to the high temperature resulting from the exothermic mineral oxidation reactions inside the leaching tank or heap. Thermophilic organisms have been increasingly used to improve mineral sulphide oxidation rates[4–5] and reduce the costs associated with the cooling of exothermic process.

Based on the great commercial importance in

hydrometallurgy of thermophilic organisms, this research was focused on screening thermophilic acidophiles from samples of acidic hot springs. A number of acidophilic thermophiles were isolated and a moderately thermophilic ferrous iron and sulphur oxidizing strain (YN22, DQ650351) has been identified as *Sulfobacillus thermosulfidooxidans*. It is the first time for this species to be isolated and identified in China.

S. thermosulfidooxidans, the most widely used moderate thermophile in sulphide mineral processing, is generally more effective than mesophilic species for sulphide mineral bioleaching. Laboratory tests showed that 22% of the available copper in chalcopyrite was rapidly released to solution via *S. thermosulfidooxidans*-mediated bioleaching, but copper leaching reaction was significantly retarded once a jarosite layer on mineral particles was formed. It has been affirmed that jarosite layer hinders copper leaching by preventing the contact between bacteria and mineral particles, restricting the mass transfer between oxidant and mineral surface[6–7].

However, the kinetics of jarosite precipitation associated with *S. thermosulfidooxidans* and the influence of jarosite precipitate on *S. thermosulfidooxidans* growth have not been previously defined. To overcome the limitation that jarosite places on metal recovery during the *S. thermosulfidooxidans*-mediated bioleaching of sulphide minerals, it is necessary to have a better understanding on the evolution of jarosite precipitation over the course of the experiment carried out under controlled conditions and the influence of jarosite on the growth of *S. thermosulfidooxidans*. The objective of this study was to characterize properties of the jarosite-type precipitates synthesized by the newly isolated strain YN22 of *S. thermosulfidooxidans* in a Fe^{2+} medium in optimal growth conditions (pH 1.5, 53 °C, 0.2 g/L yeast extract, 30 g/L $\text{FeSO}_4 \cdot 7\text{H}_2\text{O}$ and 170 r/min) and evolution of the YN22-mediated precipitation, and evaluate the influence of the precipitates on this strain. The data obtained from the study may be helpful for optimizing bioleaching parameters and improving metal recovery.

2 Experimental

2.1 Microorganism

The moderately thermophilic acidophilic strain YN22 of *S. thermosulfidooxidans* used in this study was originally isolated from an enriched hydrothermal sample of acid hot spring in Tengchong, Yunnan Province, China. The strain was G^+ regular bacillus, about 1.6–2.3 μm in length and 0.4–0.6 μm in diameter (Fig.1). It was capable of growing chemomixotrophically on Fe^{2+} or S^0 plus yeast extract (YE) at pH 1.0–2.5 with an optimum at pH 1.5 and temperatures 40–60 °C with an optimum at 53 °C. The GenBank accession number for the 16S rDNA sequence of this strain is DQ650351.

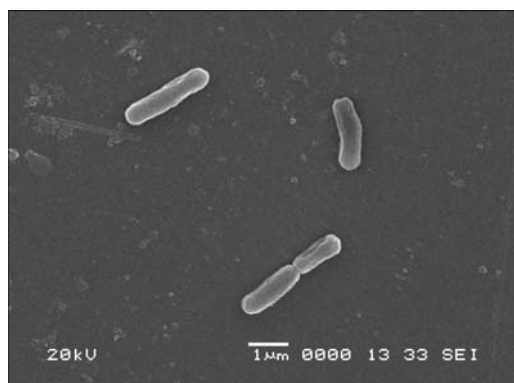


Fig.1 SEM image of YN22

The bacteria were grown at 53 °C and 170 r/min (on an orbital shaker) in a mineral salts medium with the composition of $(\text{NH}_4)_2\text{SO}_4$ (2.0 g/L), $\text{MgSO}_4 \cdot 7\text{H}_2\text{O}$ (0.3

g/L), KH_2PO_4 (0.25 g/L), KCl (0.1 g/L), yeast extract (0.2 g/L) and $\text{FeSO}_4 \cdot 7\text{H}_2\text{O}$ (30 g/L). The medium was adjusted to pH 1.5 with H_2SO_4 and autoclaved before filter-sterilized ferrous iron was added. Bacteria at steady-state were collected by centrifugation and washed twice with dilute sulfuric acid (pH 1.7) as inoculum.

2.2 Experimental method

To estimate the effect of solid particles on jarosite precipitation, glass beads (particle size between 3 and 4 mm) were used in the experiments. Before use, glass beads were treated with 5 mol/L HCl for 2 h, washed until neutral and finally autoclaved at 120 °C for 20 min.

The bacteria collected above were re-suspended ($2.9 \times 10^6/\text{mL}$) in 200 mL mineral salts medium (pH 1.5) mentioned above in 250 mL shake flasks with or without 15 g sterilized glass beads. Sterile controls with or without glass beads were carried out under the same conditions. All cultures in duplicate were performed at 53 °C and 170 r/min for measuring ferrous iron, pH value, bacterial number and jarosite-type precipitate periodically. Duplicated parallel cultures were also run under the same condition for harvesting jarosite-type precipitates in order to compare the precipitate yields between the cultures with and without glass beads.

Influence of jarosite-type precipitates on YN22 was evaluated by adding 0, 0.1, 0.2, 0.4, 0.8 and 1.0 g of the precipitates obtained from the duplicated parallel cultures with and without glass beads, to a series of 250 mL flasks containing 100 mL medium (as described above) and inoculated with a viable YN22 cell mass equivalent to $2 \times 10^6/\text{mL}$. The test duplicated and conducted under the same conditions as stated above was stopped and parameters (cell number and Fe^{2+}) were analyzed once the Fe^{2+} oxidation in the flasks added with 0 g jarosite-type precipitate reached about 97%.

2.3 Analysis method

Ferrous iron was determined by titration with $\text{K}_2\text{Cr}_2\text{O}_7$ in acid medium. pH value of solution was measured with an S-3C pH meter (Leici, Shanghai). Bacterial population density in culture supernatants was monitored by direct cell counts with a Petroff-Hauser chamber on an Olympus CX31 microscope. The cells absorbed on precipitate particles were not reckoned in the population density. Liquid samples (1 mL) were withdrawn from the flasks at regular intervals to measure the contents of jarosite-type precipitates. Before sampling, 1.5 mL microfuge tubes were freeze-dried for 5 h and weighed. The weighed tubes were then added with samples and centrifuged at 8 000 r/min for 20 min. The supernatants were discarded and the precipitate-containing tubes were freeze-dried for another 5 h and weighed again. The precipitate in each sample was

finally calculated from the difference between the two masses of the same tube. At the end of experiment, the suspended solids were obtained from the sampled flasks by centrifugation, and air dried for X-ray diffraction (XRD), scanning electron microscopy(SEM), energy dispersive spectra(EDS) and Fourier transform infrared spectra(FTIR) analyses. Precipitates in the duplicated parallel cultures, run under the same condition and never sampled, were centrifugally harvested and freeze-dried to compare the precipitate yields between the cultures with and without glass beads.

3 Results and discussion

3.1 Characterization of precipitate

Jarosite is the general name of a large number of iron-containing minerals belonging to the larger mineral family alunite, which has a common formula $M_n\text{Fe}_3(\text{SO}_4)_2(\text{OH})_6$, where M is monovalent or divalent cation such as H_3O , K, Na, NH_4 , Ag, Rb, Pb and Hg, and n is 1 or 1/2. Hydronium jarosite, ammoniojarosite, argentojarosite, natrojarosite, potassium jarosite and

plumbojarosite are the six most common jarosite minerals. These jarosite compounds are different from each other in XRD and FTIR patterns, and SEM images, depending on the composition and methods of preparation. XRD and EDS patterns indicate that the precipitates synthesized using YN22 strain of *S. thermosulfidooxidans* are potassium jarosite, with good crystallinity and all diagnostic peaks identical with potassium jarosite[8–12], as shown in Figs.2 and 3, but potassium jarosite and ammoniojarosite are difficult to be distinguished only by XRD and EDS[13].

The two biologically prepared precipitates were analyzed by FTIR for further identification. The precipitates yield similar FTIR patterns of ammoniojarosite with pronounced absorption bands at $1\,426\text{--}1\,427\text{ cm}^{-1}$ due to NH_4 deformation[14](Fig.4). And also there are distinctive IR absorbance frequencies of jarosite-type compounds in the precipitates at $1\,082\text{--}1\,199$, $1\,001\text{--}1\,003$, $472\text{--}474$, $629\text{--}630$, $506\text{--}511$, $1\,634\text{--}1\,636$ and $3\,405\text{--}3\,412\text{ cm}^{-1}$, attributed to the ν_3 vibration of SO_4 , OH deformation(σ_{OH}), τ vibration of OH, ν_4 vibration mode of SO_4 , the vibration of FeO_6 ,

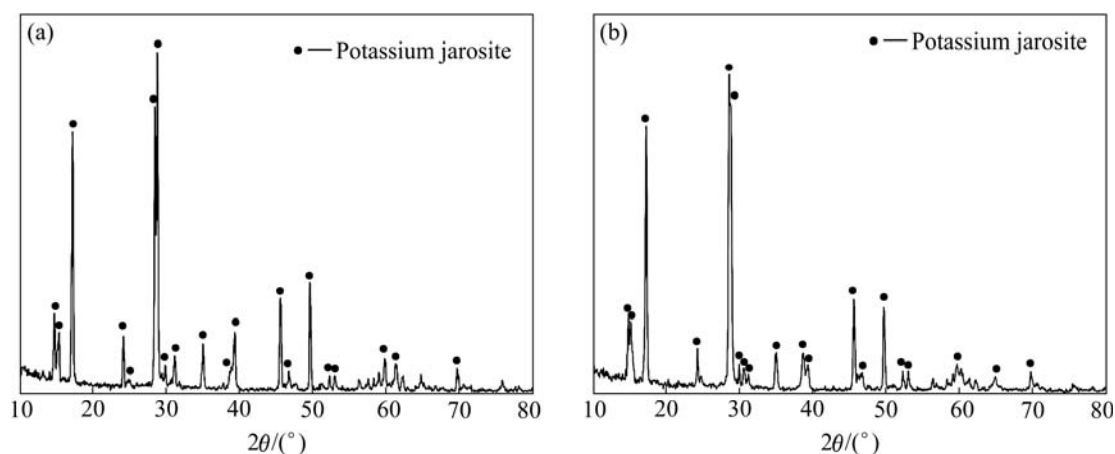


Fig.2 XRD patterns of YN22-mediated precipitates: (a) Without glass beads; (b) With glass beads

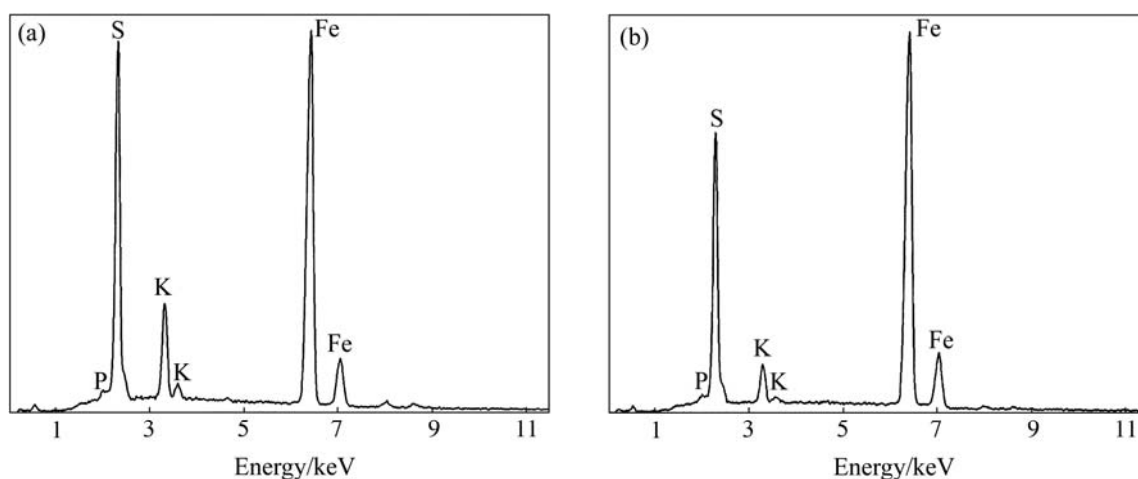


Fig.3 EDS patterns of YN22-mediated precipitates: (a) Without glass beads; (b) With glass beads

HOH deformation and OH stretching[13,15] respectively, as shown in Fig.4.

As reported previously, morphological features of jarosite-type compounds were found to be different from each other, mainly depending on the method of preparation and the nature of the monovalent cation. SASAKI and KONNO[8] used several methods to form jarosite-type compounds, including biologically mediated formation by *Acidithiobacillus ferrooxidans* at 30 °C and chemical formations at slow and rapid oxidation of Fe^{2+} by H_2O_2 at the same temperature. The products of potassium jarosite consisted of round and granular particles without sharp edges, whereas the

products of ammoniojarosite were characterized by cubic particles with well developed sharp edges, though the particles of chemically synthesized ammoniojarosite are much larger in size and better developed in planar facets than those of biologically formed product. The two precipitates formed using strain YN22 are similar in morphology to the products of ammoniojarosite mentioned above. The precipitate formed by strain YN22 with glass beads looks like the *A. ferrooxidans*-formed ammoniojarosite (Figs.5(a) and (b)), which has less aggregated small particles, and the precipitate formed by strain YN22 without glass beads is almost the same as the ammoniojarosite chemically synthesized at a rapid

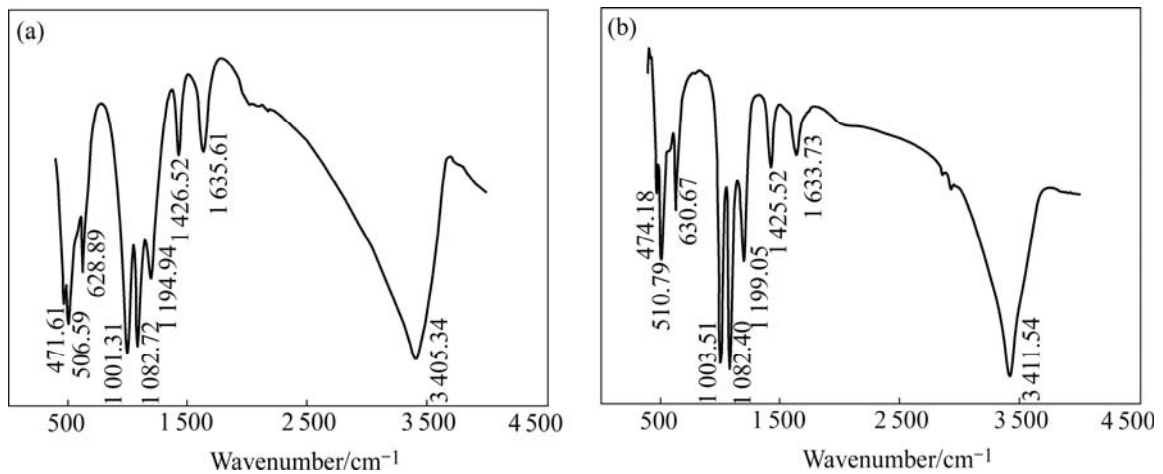


Fig.4 FTIR patterns of YN22-mediated precipitates: (a) Without glass beads; (b) With glass beads

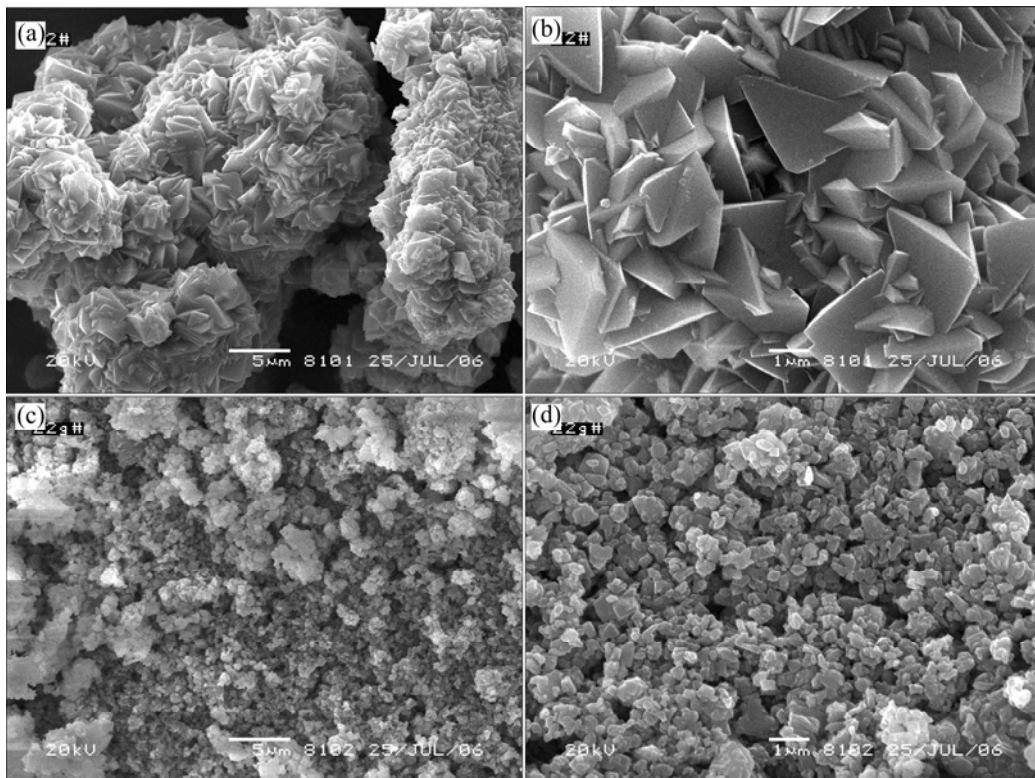


Fig.5 SEM images of YN22-mediated precipitates: (a), (b) Without glass beads; (c), (d) With glass beads

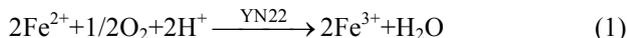
rate of Fe^{2+} oxidation, consisting of aggregates of large cubic particles with fully developed sharp edges and planar facets (Figs.5(c) and (d)).

The differences between the two YN22-formed precipitates are considered to be caused by the glass beads that break large particles into small pieces and therefore prevent the formation of large crystal in the flask with glass beads.

The data from XRD, EDS, FTIR and SEM suggest that the precipitates formed using strain YN22 of *S. thermosulfidooxidans* at 53 °C are the mixture of potassium jarosite and ammoniojarosite, with morphological features similar to the latter.

3.2 Precipitation evolution

YN22 is a very active iron metabolizing strain of *A. thermosulfidooxidans* and capable of oxidizing more than 90% of Fe^{2+} within 30 h when being added with 30 g/L $\text{FeSO}_4 \cdot 7\text{H}_2\text{O}$ under the controlled experimental conditions. Jarosite-type precipitates were first observed in the YN22-inoculated flasks, where over 97% of Fe^{2+} was oxidized, after 32 h of inoculation for the flasks with glass beads and 38 h for the flasks without glass beads. This precipitation reaction coupled with YN22-mediated oxidization of Fe^{2+} can be described as follows:



where R is monovalent cation K^+ or NH_4^+ .

Fig.6 demonstrates the propensities of the precipitation to change concurrent with the evolutions of Fe^{2+} , pH value and bacterial population density. Precipitates increase stepwise from 6.6 g/L (at 32 h) to 14.4 g/L (at 100 h) in the YN22-inoculated flasks with glass beads and from 4.3 g/L (at 38 h) to 8.1 g/L (at 94 h) in the YN22-inoculated flasks without glass beads. The experimentation is ended when precipitate no longer increases (at 110 h). There are remarkable differences in the oxidation rate of Fe^{2+} and the yield of jarosite-type precipitate between the two groups of cultures, 6 h faster for oxidation of Fe^{2+} , 6 h earlier for precipitation and 78% higher for precipitate yield in the flasks containing glass beads than in those without glass beads (Fig.6(a)).

Nevertheless, in contrary to the YN22-inoculated cultures, no precipitate is found in the sterile controls with or without glass beads throughout the course of the experimentation (total 110 h), therefore no datum of the sterile controls is involved in the discussion.

The pH values rise gradually from 1.50 to the highest points of 1.82 in the flasks with glass beads and 1.89 in the flasks without glass beads as Fe^{2+} decreases from 6.0 g/L to 0.2 g/L. Hereafter, pH values are

changed in a contrary manner, down from 1.82 or 1.89 to 1.20 (with glass beads) or 1.42 (without glass beads) with precipitate accumulation (Fig.6(b)). This propensity of pH evolution can be well expounded by the above reactions 1 and 2. H^+ is consumed in the YN22-mediated reaction 1, in which Fe^{2+} is oxidized to Fe^{3+} and pH value increases until precipitate occurs. Contrarily,

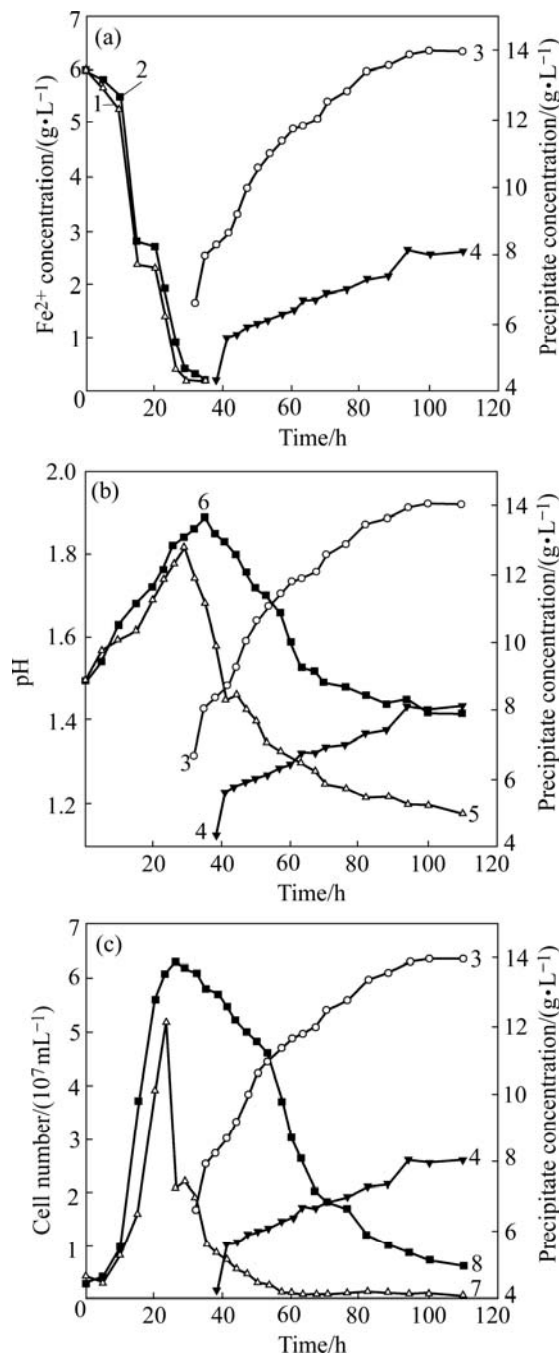


Fig.6 Precipitation propensities to change concurrent with evolutions of Fe^{2+} (a), pH (b) and bacterial population density (c): 1 Fe^{2+} (with glass beads); 2 Fe^{2+} (without glass beads); 3 Precipitate (with glass beads); 4 Precipitate (without glass beads); 5 pH (with glass beads); 6 pH (without glass beads); 7 Cell (with glass beads); 8 Cell (without glass beads)

H^+ is released into the solution in reaction 2, in which pH value decreases until the precipitation is terminated. The strong precipitation in the flasks with glass beads could create a pH value as low as 1.20, much lower than that (1.42) in the flasks without glass beads and very detrimental to the growth of YN22.

When being added with $FeSO_4 \cdot 7H_2O$ as the unique energy source and inoculated on optimal conditions, YN22 oxidizes Fe^{2+} quickly and gets the energy necessary for supporting its rapid growth. The population densities in the flasks both with and without glass beads undergo a similar population evolution, increasing expeditiously along with Fe^{2+} oxidation and decreasing with precipitate piling up, though the population densities in the flasks with glass beads drop very sharply during the initial period of precipitation (Fig.6(c)).

Precipitation of ammoniojarosite or potassium jarosite consumes NH_4^+ or K^+ [16], which is indispensable to the growth of YN22, and releases H^+ into ambient solution, causing pH to go down. A great amount of jarosite-type precipitate deposited in the glass bead-added flasks led to a great consumption of NH_4^+ and K^+ , and a sharp drop of pH value, which were unfavorable for growth of the YN22 bacteria in these flasks. On the other hand, some suspending bacteria were absorbed to or wrapped in precipitate particles. As a result, these bacteria were settled out of liquid media and not reckoned in the recorded bacterial population densities in all YN22-noculated flasks. However, much more precipitate was produced and therefore a greater number of bacteria were co-deposited in the flasks with glass beads than in those free of glass beads. These were the main reasons why bacterial number of YN22 appeared to be much smaller in the glass bead-added flasks compared with the flasks free of glass beads throughout the period subsequent to the time when precipitates occurred. Except available Fe^{2+} concentration, pH value and jarosite-type precipitation, another factor that affected YN22 population density was the shearing force originated from the swiveling of glass beads, which maybe retard the growth of YN22 population at 170 r/min significantly.

3.3 Influence of jarosite-type precipitates on strain YN22

An aspect of the concentration gradient study of precipitate was conducted to evaluate the response of strain YN22 to the two jarosite-type precipitates obtained from the duplicated parallel flasks both with and without glass beads. The data referring to the growth and Fe^{2+} oxidation rate of strain YN22 in the media plus different concentrations of the jarosite-type precipitates are presented in Fig.7. There is little difference detected in

Fe^{2+} oxidation rate among the cultures containing the precipitate originated from the flasks without glass beads. However, the cultures added with the highest concentration (10 g/L) of the precipitate have a little lower Fe^{2+} oxidation rate compared with the other cultures (Fig.7(a)), and increasing precipitate concentration causes a gently decreasing in population density (Fig.7(b)). Contrary to the data above, YN22 is susceptible to the precipitate obtained from the flasks with glass beads, with a sharp decrease in population density and a rapid decline in Fe^{2+} oxidation rate when being added with the precipitate over 4 g/L (Fig.7). Considering the chemical identity of the precipitates revealed by XRD, FTIR and EDS, it is possible that some physical differences between the two precipitates used in this study result in different responses of strain YN22 to these precipitates. However, a further study is needed to find the certain factors that lead to this phenomenon.

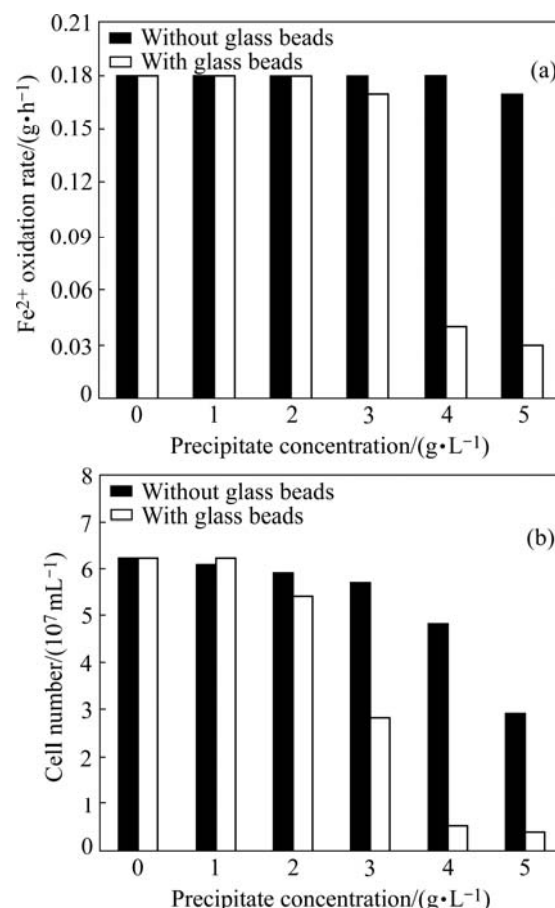


Fig.7 Influences of strain YN22-mediated precipitates on Fe^{2+} oxidation rate (a) and growth (b) of YN22

4 Conclusions

1) Remarkable differences are observed in the oxidation rate of Fe^{2+} , the yield of precipitate and the density of bacterial population between the two groups

of cultures. The group with glass beads has a 6 h faster Fe^{2+} oxidation, 6 h earlier precipitation, 78% higher precipitate yield and much lower population density than those without glass beads.

2) XRD, EDS, FTIR and SEM analyses reveal that the precipitates originated from both groups are a mixture of potassium jarosite and ammoniojarosite, with morphological features similar to the latter. The precipitate from the cultures free of glass beads places no apparent influence on Fe^{2+} oxidation rate of YN22 and only a limited influence on growth of the strain, whereas that from glass bead-added cultures remarkably inhibits the growth and Fe^{2+} oxidation ability of YN22 when a precipitate content over 4 g/L is used.

3) The factors that affect YN22 may result from some physical features of the precipitate, but a further study is needed to find the real causes for this phenomenon.

References

- [1] WITNE J Y, PHILLIPS C V. Bioleaching of Ok Tedi copper concentrate in oxygen and carbon dioxide-enriched air [J]. *Minerals Engineering*, 2001, 14(1): 25–48.
- [2] KREBS W, BROMBACHER C, BOSSHARD P P, BACHOFEN R, BRANDL H. Microbial recovery of metals from solids [J]. *FEMS Microbiol Rev*, 1997, 20(3/4): 605–617.
- [3] BOSECKER G K. Bioleaching: Metal solubilization by microorganisms [J]. *FEMS Microbiol Rev*, 1997, 20(3/4): 591–604.
- [4] ROBERTSON W J, KINNUNEN P H-M, PLUMB J J, FRANZMANN P D, PUHAKKA J A, GIBSON J A E, NICHOLS P D. Moderately thermophilic iron oxidizing bacteria isolated from a pyretic coal deposit showing spontaneous combustion [J]. *Minerals Engineering*, 2002, 15: 815–822.
- [5] CLARK D A, NORRIS P R. Oxidation of mineral sulphides by thermophilic microorganisms [J]. *Minerals Engineering*.1996, 9 (11): 1119–1125.
- [6] HILTUNEN P, VUORINEN A, REHTIJARVI P, TUOVINEN O H. Bacterial pyrite oxidation: Release of iron and scanning electron microscopic observations [J]. *Hydrometallurgy*, 1981, 7(1/2): 147–157.
- [7] BOON M, HEIJNEN J J. Mechanisms and rate limiting steps in bioleaching of sphalerite, chalcocopyrite and pyrite with *Thiobacillus ferrooxidans* [C]// TORMA A E, WEY J E, LAKSHMANAN V I. *Biohydrometallurgical Technologies (Volume I)*. Pennsylvania: TMS, 1993: 217–235.
- [8] SASAKI K, KONNO H. Morphology of jarosite-group compounds precipitated from biologically and chemically oxidized Fe ions [J].*The Canadian Mineralogist*, 2000, 38: 45–56.
- [9] BEVILAQUA D, LEITE A L L C, GARCIA O, TUOVINEN O H. Oxidation of chalcocopyrite by *Acidithiobacillus ferrooxidans* and *Acidithiobacillus thiooxidans* in shake flasks [J]. *Process Biochemistry*, 2002, 38: 87–592.
- [10] MIN Xiao-bo, CHAI Li-yuan, CHEN Wei-liang, ZHANG Chuan-fu, ZHONG Hai-yun, KUANG Zhong. Bioleaching of refractory gold ore (II): Mechanism on bioleaching of arsenopyrite by *Thiobacillus ferrooxidans* [J]. *Trans Nonferrous Met Soc China*, 2002, 12(1): 142–146.
- [11] SHI Shao-yuan, FANG Zhao-heng. Bioleaching of marmatite flotation concentrate by *Acidithiobacillus ferrooxidans* and *Leptospirillum ferrooxidans* [J]. *Trans Nonferrous Met Soc China*, 2004, 14(3): 69–575.
- [12] ASOKAN P, SAXENA M, ASOLEKAR S R. Jarosite characteristics and its utilisation potentials [J]. *Science of the Total Environment*, 2006, 359: 32–243.
- [13] BIGHAM J M, BHATTI T M, VUORINEN A, TUOVINEN O H. Dissolution and structural alteration of phlogopite mediated by proton attack and bacterial oxidation of ferrous iron [J]. *Hydrometallurgy*, 2001, 59: 301–309.
- [14] LAZAROFF N, WASSERMAN A. Iron oxidation and precipitation of ferric hydroxysulfates by resting *Thiobacillus ferrooxidans* cells [J]. *Appl Environ Microbiol*, 1982, 43: 24–938.
- [15] DROUET C, NAVROTSKY A. Synthesis, characterization, and thermochemistry of K-Na-H₂O jarosites [J]. *Geochimica et Cosmochimica Acta*, 2003, 67(11): 2063–2076.
- [16] ZHANG Guang-ji, FANG Zhao-heng. Behavior of Fe and S in bioleaching of pentlandite [J]. *Trans Nonferrous Met Soc China*, 2002, 12(1): 160–163.

(Edited by LI Xiang-qun)